Supplementary Material

1 SUPPLEMENTARY FIGURES

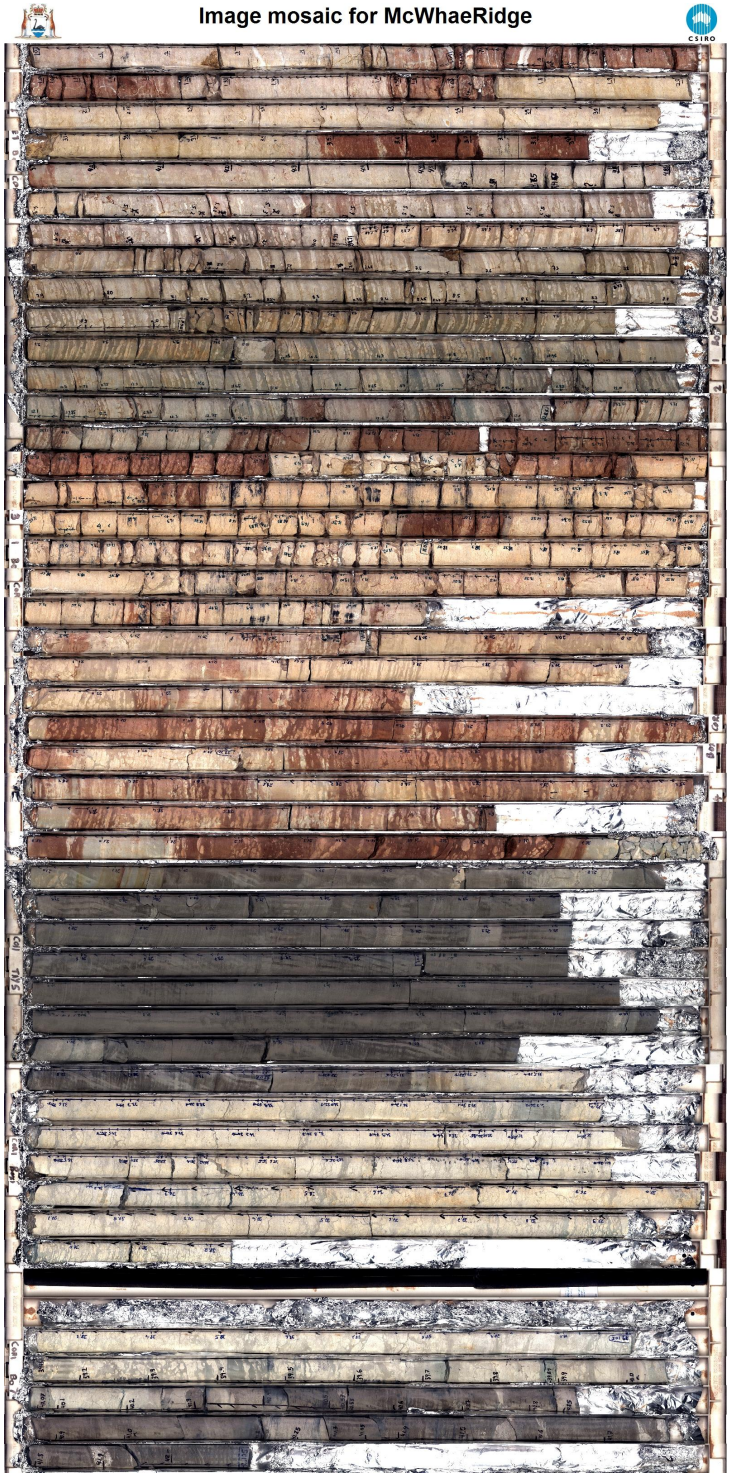

Figure S1. MR1 core Image mosaic of the McWhae Ridge Winkie core. Upper left corner is the top of the core, and lower right is the bottom.

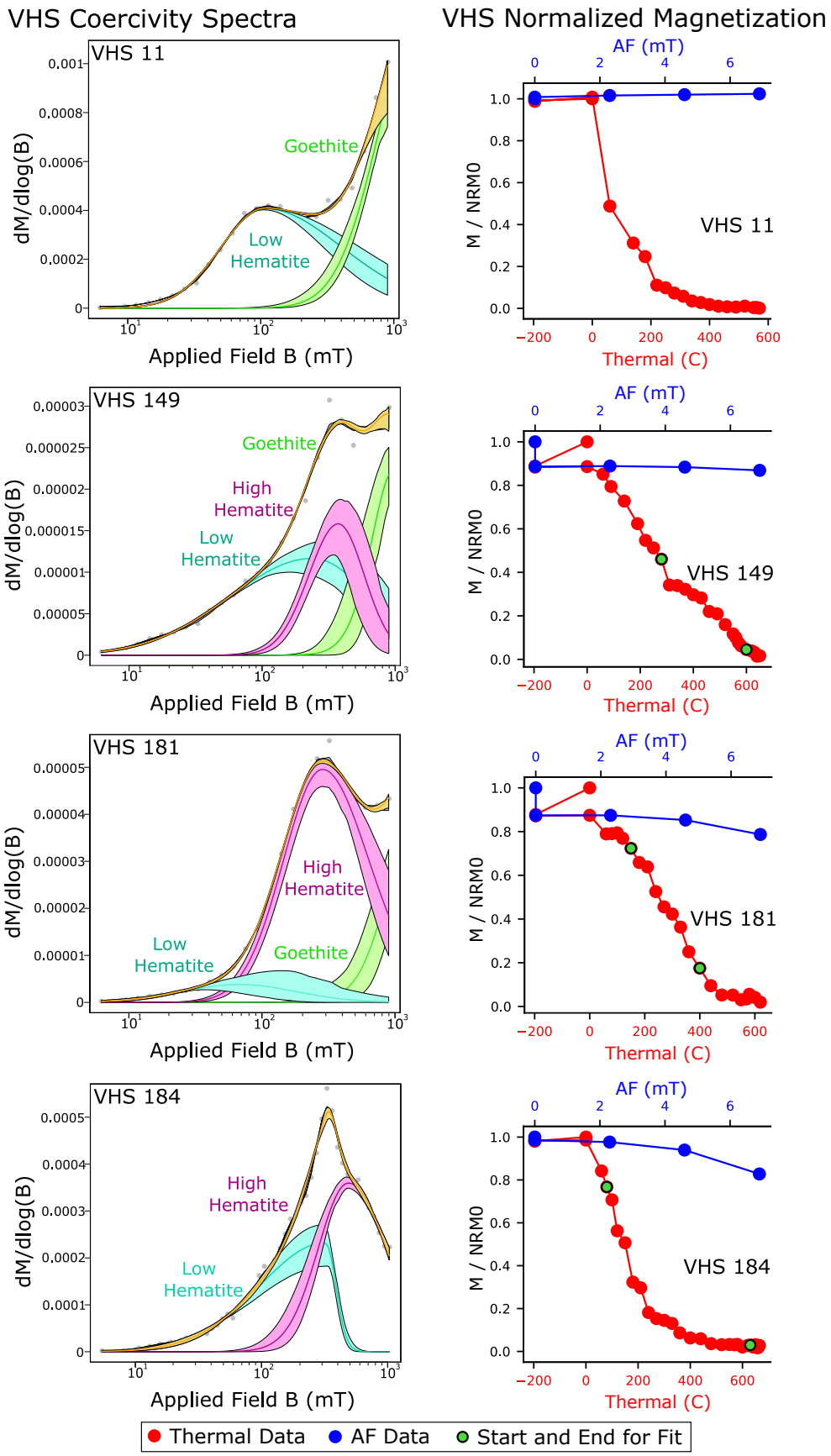
VHS Coercivity Spectra
VHS Normalized Magnetization
VHS 11
Goethite
Low Hematite
dM/dlog(B)
Applied Field B (mT)
AF (mT)
M / NRM0
Thermal (C)
VHS 149
High Hematite
VHS 181
VHS 184
Thermal Data
AF Data
Start and End for Fit

Figure S2. Unmixed magnetic components for VHS samples Rock magnetic data were collected for four samples in the VHS section (Hansma et al., 2015). The plots in the left column show the magnetic mineral components contained in those samples, made using MAX UnMix (Maxbauer et al., 2016). The samples were fit with three components, with each sample containing some combination of two or three of these magnetic minerals. The 143-173 mT component was interpreted as low-coercivity hematite potentially pigmentary hematite (Swanson-Hysell et al., 2019) and was found in all four samples. The 278-548 mT component was interpreted as high-coercivity hematite and was found in three samples. The 1050-1440 mT component was interpreted as goethite and was found in three samples. The plots in the right column show the magnetization normalized to initial magnetization (M/NRM0) for each of the samples. The green dots show the start and end of the characteristic remanent magnetization (ChRM) component fit for samples VHS 149, VHS 181, and VHS 184 from Hansma et al. (2015). Notably, similar to MR1, samples with a ChRM are from those containing high-coercivity hematite (potentially detrital); interestingly, most paleomagnetic fits focus on low-temperature demagnetization regions that could be due to pigmentary hematite or non-stoichiometric magnetite identified in the low-coercivity hematite component.

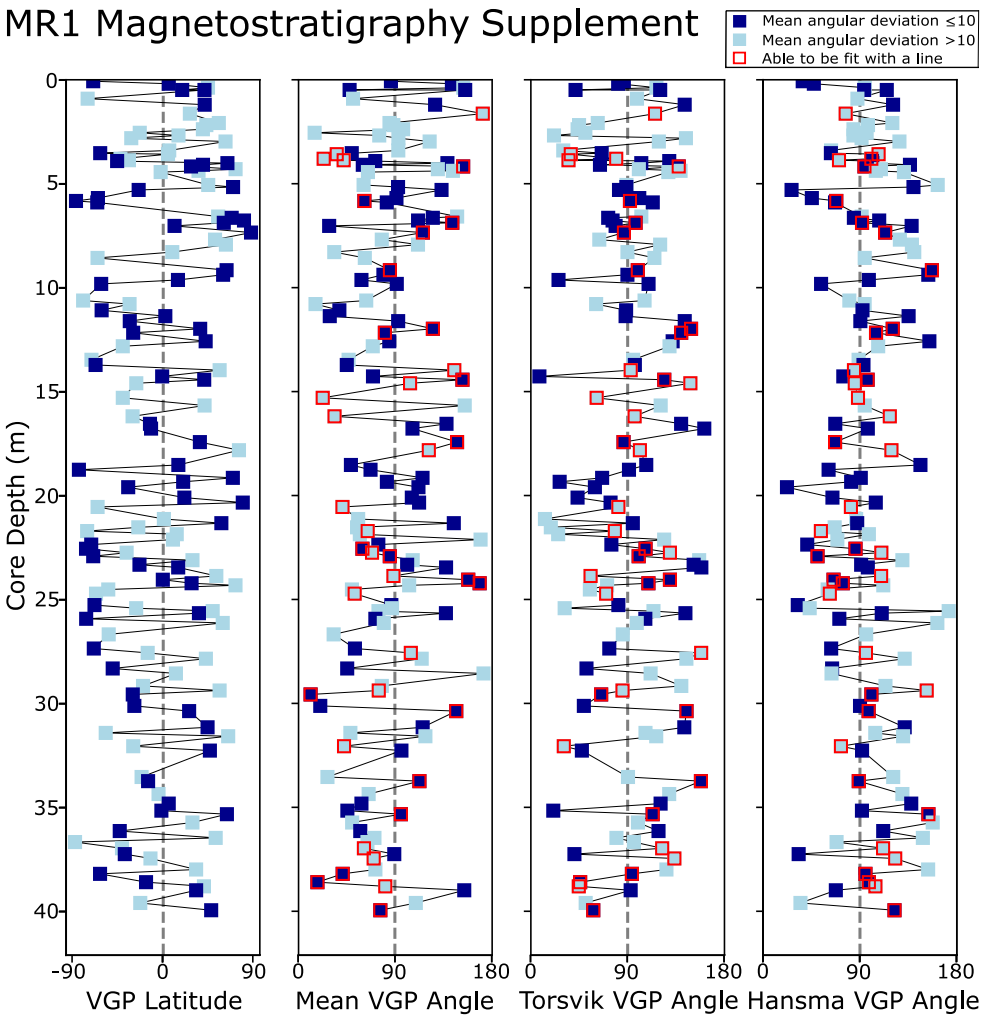

Figure S3. Comparison of VGP angles for MR1 In the first column, virtual geomagnetic pole (VGP) latitude data is plotted stratigraphically for the high-temperature components of MR1. In the following columns, VGPs are plotted as an angle from each of three poles: the mean VGP of the dataset, the paleopole calculated by Torsvik et al. (2012) for Gondwana at 370 Ma, and the paleopole calculated by Hansma et al. (2015) for the Canning Basin. The magnetic reversals determined from each of these different datasets were used to create a corresponding magnetostratigraphic record (Figure 4). The samples that could be fit with a line going to the origin instead of an anchored line are outlined in red on the VGP plots.

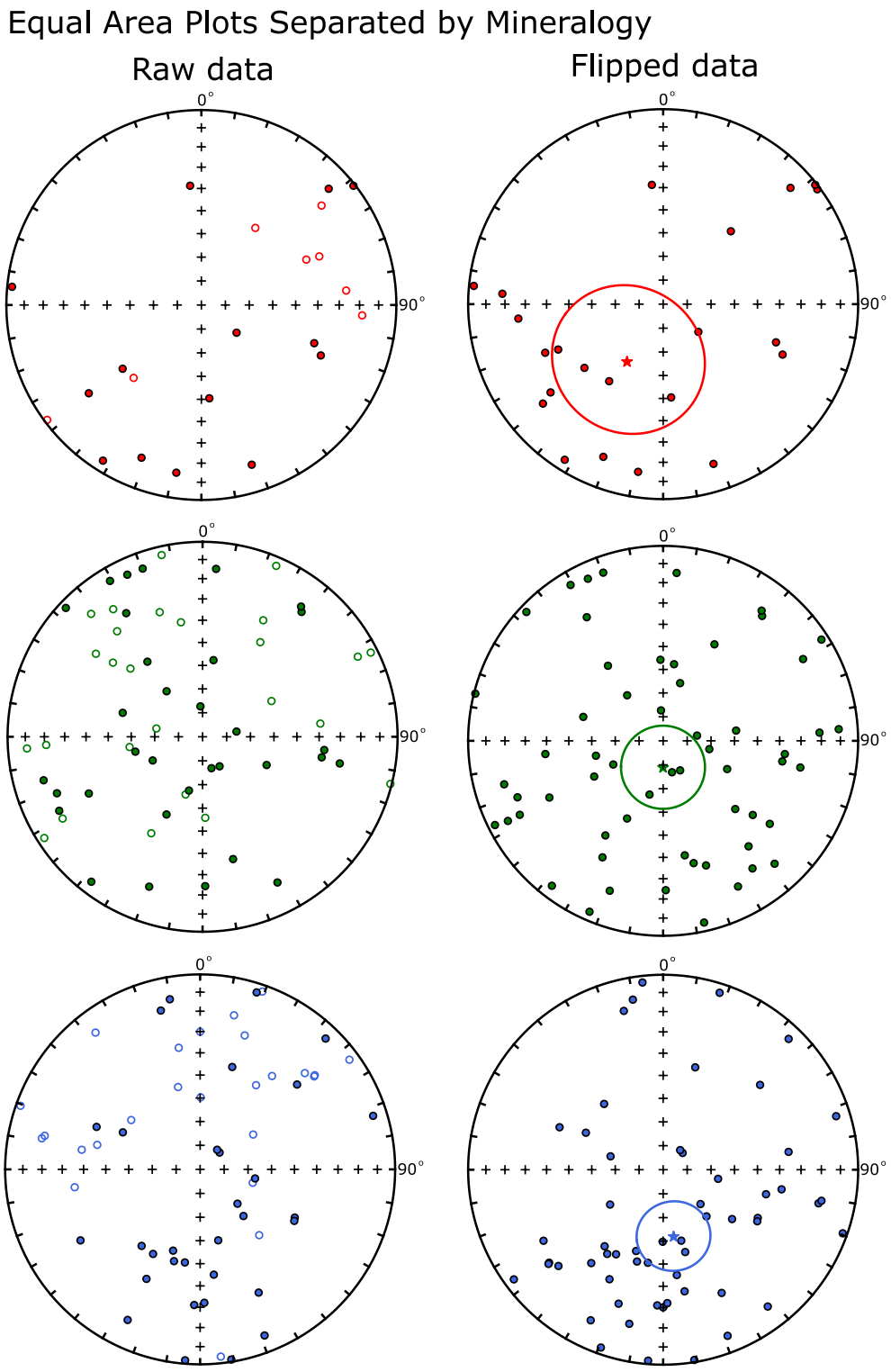

Figure S4. High-temperature paleomagnetic directions for MR1 samples separated by mineralogy Equal area plots for high-temperature components separated by interpretations of mineralogy based on blocking temperature (red: hematite, green: pyrrhotite, blue: magnetite). Left column has raw data, right column has data flipped such that all points are in the same hemisphere. Hematite Fisher mean: D=212.1°, I=61.4°, α95=31.7, n=22 (Tilt-corrected coordinates). Pyrrhotite Fisher mean: D=180.2°, I=78.9°, α95=17.4, n=59 (Tilt-corrected coordinates). Magnetite Fisher mean: D=171.1°, I=61.6°, α95=14.9, n=57 (Tilt-corrected coordinates).

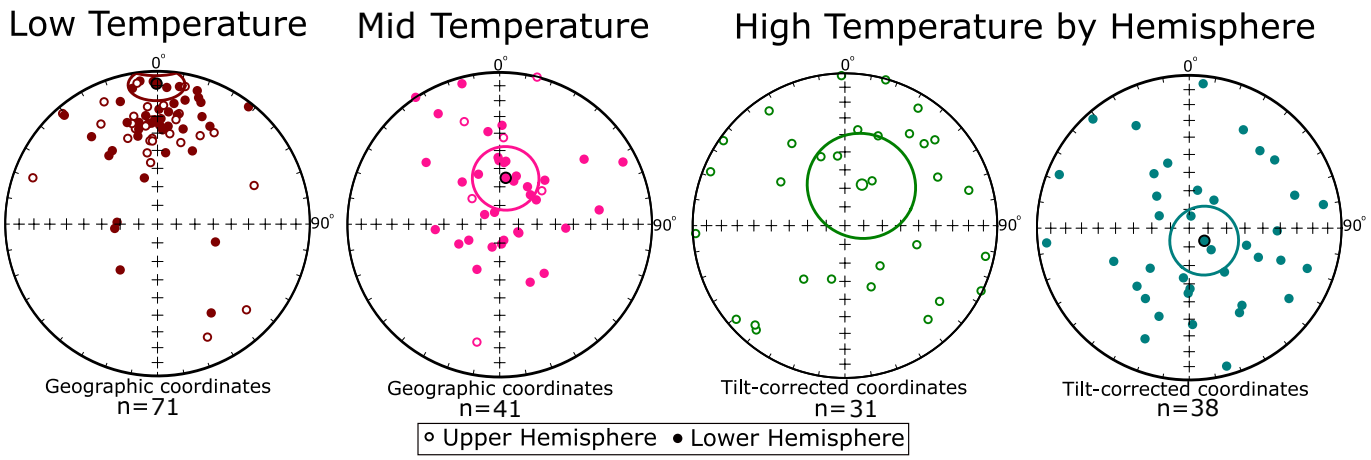

Figure S5. Paleomagnetic Directions for WK1 samples Equal area plots for low-temperature components, mid-temperature components, and high-temperature components, separated into upper and lower hemispheres. The low-temperature fits have a well-clustered mean direction (D=359.6°, I=-5.4°, α95=11.5, n=71. Geographic coordinates), but it seems to be a mix of the present local field and a reversed direction, perhaps the mid-overprint. The mid-temperature fits are mainly in a reversed direction (Fisher mean D=4.3°, I=51.1°, α95=17.4, n=41. Geographic coordinates); notably, the virtual geomagnetic pole direction does not align with the Kiaman-aged overprints (Torsvik et al., 2012). The high-temperature fits show two different clusters, separated by hemisphere (Upper Hemisphere Fisher mean D=22.5°, I=-66.2°, α95=28.7, n=31. Lower Hemisphere Fisher mean D=129.9°, I=79.5°, α95=18.4, n=38. Tilt-corrected coordinates).

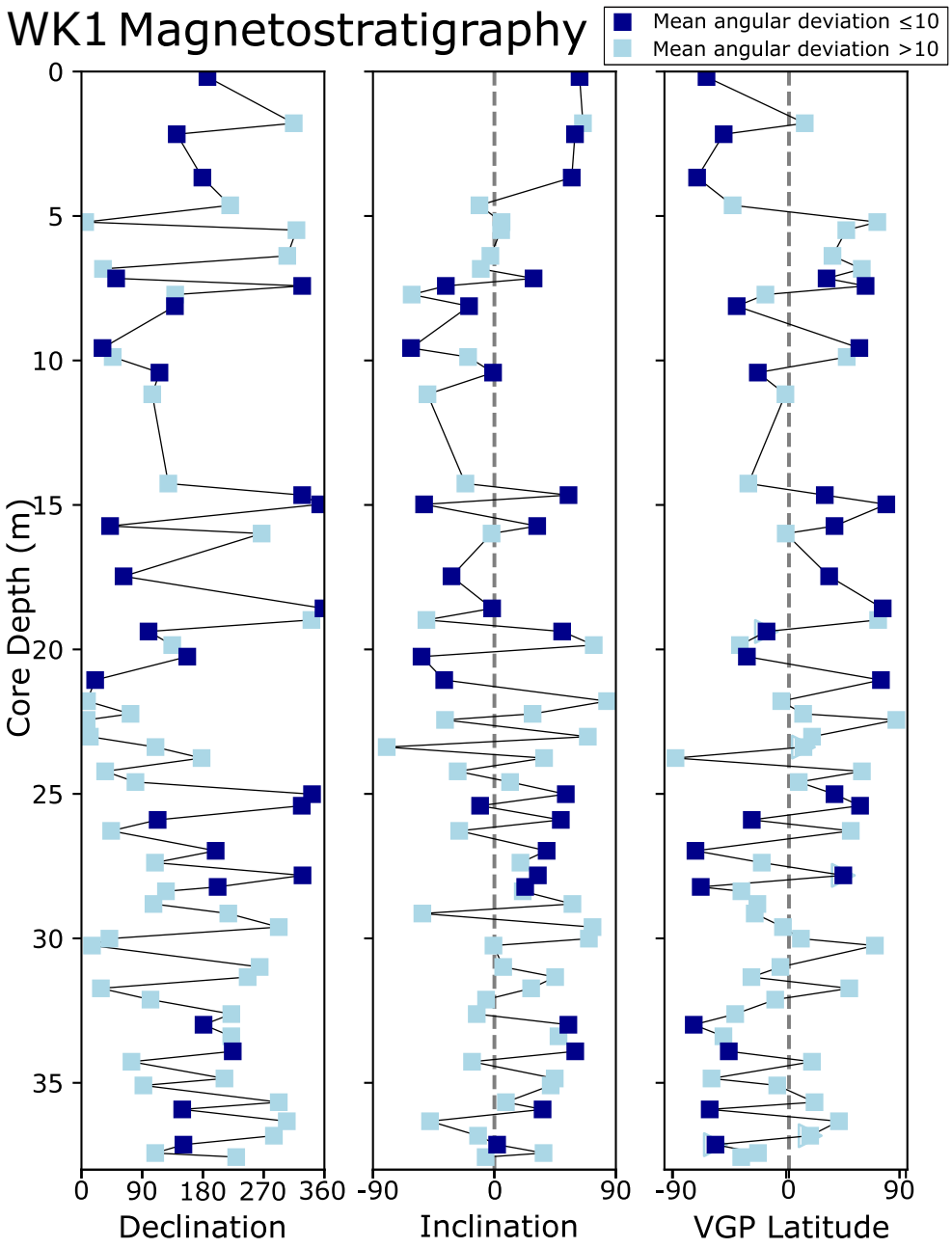

Figure S6. Paleomagnetic directional data for WK1 Declination, inclination, and virtual geomagnetic pole (VGP) latitude data for the high-temperature components of WK1.

2 SUPPLEMENTARY TABLE

Start Meterage	End Meterage	Polarity (Hansma VGP Angle)
0	0.4	Reversed
0.4	2.25	Normal
2.25	3.25	Uncertain
3.25	3.6	Reversed
3.6	5.3	Normal
5.3	6.75	Reversed
6.75	9.75	Normal
9.75	11.0	Reversed
11.0	13.3	Normal
13.3	15.6	Uncertain
15.6	18.6	Normal
18.6	23.0	Reversed
23.0	24.0	Normal
24.0	25.4	Reversed
25.4	28.1	Normal
28.1	28.9	Reversed
28.9	38.75	Normal
38.75	40.0	Reversed

Table S1. Meterage of polarity changes for Hansma VGP angle The ”Hansma” magnetostratigraphy in Figure 4 is an interpretation of the VGP angle data, derived from the paleopole calculated by Hansma et al. (2015) and shown in the same figure (fifth column). The specific meterages of the polarity chrons in that magnetostratigraphic record are detailed in this table.

REFERENCES

Hansma, J., Tohver, E., Yan, M., Trinajstic, K., Roelofs, B., Peek, S., et al. (2015). Late Devonian carbonate magnetostratigraphy from the Oscar and Horse Spring Ranges, Lennard Shelf, Canning Basin, Western Australia. *Earth and Planetary Science Letters* 409, 232–242

Maxbauer, D. P., Feinberg, J. M., and Fox, D. L. (2016). MAX UnMix: A web application for unmixing magnetic coercivity distributions. *Computers & Geosciences* 95, 140–145

Swanson-Hysell, N. L., Fairchild, L. M., and Slotznick, S. P. (2019). Primary and secondary red bed magnetization constrained by fluvial intraclasts. *Journal of Geophysical Research: Solid Earth* 124, 4276–4289. doi:https://doi.org/10.1029/2018JB017067

Torsvik, T. H., Voo, R. V. d., Preeden, U., Niocaill, C. M., Steinberger, B., Doubrovine, P. V., et al. (2012). Phanerozoic polar wander, palaeogeography and dynamics. *Earth-Science Reviews* 114, 325–368